Arab Journal of Nuclear Science and Applications, 48(4), (67-75) 2015

Calibration of Cylindrical NaI(Tl) Detector Using Different Perpendicular Radioactive Cylindrical Sources

Mohamed. S. Badawi
Physics Department, Faculty of Science, Alexandria University, 21511 Alexandria, Egypt.

Received: 3/1/2015 **Accepted: 12/5/2015**

ABSTRACT

Environmental samples containing some contaminated samples of a wide variety of characteristics are routinely analyzed using gamma-ray detectors. In this work the full energy peak efficiency of NaI(Tl) scintillation detectors 2"x2" and 3"x3" inches have been calculated experimentally by using perpendicular radioactive cylindrical sources and theoretically by applying an analytical efficiency transfer expression. This expression was based on including the ratio of the source-to-detector effective solid angle. Measurements were made using the perpendicular cylindrical vials filled with 152Eu solution. The Calibration process covers a wide energy range starting from 121 up to 1408 keV. In addition, the self-attenuation factor was estimated by using the linear attenuation factor of the assayed source material and the geometrical configuration of the assay set-up at low source-detector distance. A remarkable agreement between measured and calculated efficiency values was observed.

Keywords: Full-energy peak efficiency/Scintillation detector/ Efficiency transfer.

INTRODUCTON

Studying the detector efficiency is very important, especially in the field of activation analysis, many authors [1-9] have been calculated the full-energy peak efficiency of different detector taking into account the self-attenuation of source material. *Selim and Abbas* [10-16] using spherical coordinate system derived direct analytical integrals to calculate detector efficiencies for any source-to-detector configuration. Moreover, they introduced a new theoretical approach based on that direct Statistical method to determine the detector efficiency for an isotropic radiating point source at any arbitrary position from a cylindrical detector, as well as the extension of this approach to evaluate the volumetric sources. Where the knowledge of the solid angle subtended by the detector is essential for the calculation of full-energy peak efficiency.

In this work, the full-energy peak efficiency (FEPE) of a cylindrical NaI(Tl) detector has been calculated using perpendicular radioactive cylindrical sources using the efficiency transfer principle. The efficiency transfer principle was used before by several authors [17-23] to calculate the detector efficiency. The self attenuation coefficient of the source materials, all absorbers between the source and the detector active medium have been taken into account in calculating the effective solid angle between the source and the detector. The calculated full-energy peak efficiencies have been compared with experimental one, where the experimental part that presented in this work has been done in Prof. Dr. Younis. S. Selim laboratory for Radiation Physics, Faculty of Science, Alexandria University, Alexandria, Egypt.

MATHEMATICAL VIEWPOINT

The effective solid angle of a point source that placed at a distance, h, on the axis of the cylindrical shape detector is given as the following equation taking into account the attenuation factors of all absorbers between the source and the detector.

$$\Omega_{eff(Point)} = \int_{\theta}\int_{\varphi} f_{att}.\,(1\text{-}e^{-\mu.d_i})\,\sin\theta d\varphi d\theta \qquad (1)$$

where, f_{att}, factor determining the photon attenuation by all absorbers between source and detector (like source holder, detector end cap material, and Aluminum oxide reflector) which given as:

$$f_{att} = e^{-\sum_i \mu_i \delta_i} \qquad (2)$$

Where, μ_i, is the attenuation coefficient for a gamma-ray photon with energy, E_γ , and ,δ_i, is the average gamma photon path length through the, i^{th}, absorber.

Also, d_i, is the possible pass lengths of photon inside the detector active medium where, i, takes the values 1 and 2 where, d_1, represents the possibility of photons to enter the detector active medium from its face and exit from its base, also, d_2, represents the possibility of photons to enter the detector active medium from its face and exit from its side [6]. The pass lengths d_1 and d_2 are described as the following equation:

$$d_1 = \frac{L}{\cos(\theta)} \quad \text{and} \quad d_2 = \frac{R}{\sin\theta} - \frac{h}{\cos\theta} \qquad (3)$$

where, L, is the detector side length, R, is the detector Radius, h, is the separation distance between source and detector.

The pass lengths of the photon inside the detector material are controlled by polar and azimuthal angles θ and ϕ and defined as the following:

$$\theta_1 = \tan^{-1}\left(\frac{R}{L+h}\right) \quad \text{and} \quad \theta_2 = \tan^{-1}\left(\frac{R}{h}\right) \qquad (4)$$

where, ϕ changes from 0 to 2π. Also, if the incidence angle θ less than θ_1, then the photon pass length will be, d_1, also if θ less than θ_2 and greater than θ_1, then the photon pass length will be, d_2.

Any volumetric shape source of volume, V, can be treated as a group of point sources which are uniformly distributed; each point source has the effective solid angle, $\Omega_{eff(Point)}$ as the following equation:

$$\Omega_{eff\,(Vol)} = \frac{\int_v f_{att}.\,\Omega_{eff\,(Point)}\; dV}{V} \qquad (5)$$

To determine the effective solid angle of cylindrical source perpendicular of radius, S, and of height, 2a less than the radius of the detector subtended with the cylindrical detector (S<R), centered to be perpendicular on the detector's axis as shown in Figure (1) [6], the source is divided into a very thin rectangle layers, which have homogeneously radioactive distributed area. Therefore, the solid angle of a co-axial cylindrical detector, $\Omega_{Cyl\text{-}Per}$, can be given as:

$$\Omega_{(Cyl-Per)} = \frac{\int_{h_o}^{2S+h_o} [\int_0^{\alpha_1}\int_0^{\rho_1} \Omega_{(Point)}\rho d\rho d\alpha + \int_{\alpha_1}^{\pi-\alpha_1}\int_0^{\rho_2} \Omega_{(Point)}\rho d\rho d\alpha + \int_{\pi-\alpha_1}^{\pi}\int_0^{\rho_1} \Omega_{(Point)}\rho d\rho d\alpha]\, dh}{\pi S^2 a} \quad (6)$$

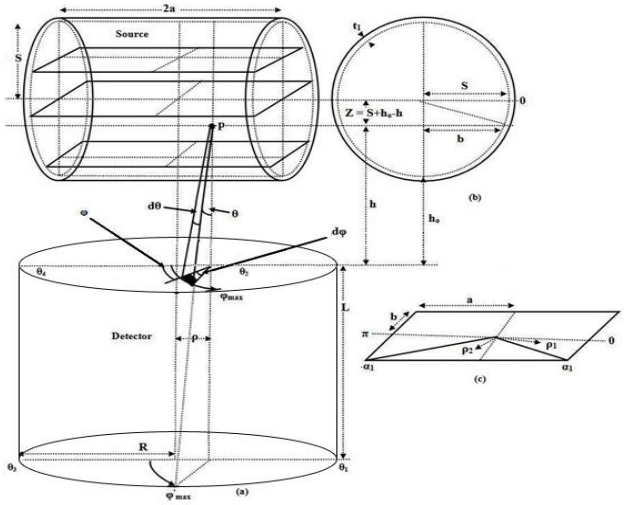

Fig.(1): Perpendicular cylindrical source with respect to Co-axial cylindrical detector: (a) source–detector configuration, (b) source vertical plane and (c) source horizontal plane.

The source self-attenuation coefficient, S_f is given by:

$$S_f = e^{-\mu_s . d_s} \quad (7)$$

where, μ_s, is the source attenuation coefficient and, d_s, the distance traveled by the photon inside the source material is given by:

$$d_s = \frac{(B - A)}{C} \quad (8)$$

where,

$$\left.\begin{aligned} A &= (Z\ \cot\theta + \rho\ \sin\alpha\ \sin\varphi) \\ B &= \sqrt{A^2 - (\sin^2\varphi + \cot^2\theta)(Z^2 - S^2 + \rho^2\sin^2(\alpha))} \\ C &= (\sin^2\varphi + \cot^2\theta)\sin\theta \end{aligned}\right\} \quad (9)$$

So, the effective solid angle for perpendicular cylindrical source equation will be:

$$\Omega_{eff(Cyl\text{-}Per)} = \frac{\int_{h_o}^{2S+h_o} [\int_0^{\alpha_1}\int_0^{\rho_1} S_f . \Omega_{eff(Point)}\rho d\rho d\alpha + \int_{\alpha_1}^{\pi-\alpha_1}\int_0^{\rho_2} S_f . \Omega_{eff(Point)}\rho d\rho d\alpha + \int_{\pi-\alpha_1}^{\pi}\int_0^{\rho_1} S_f . \Omega_{eff(Point)}\rho d\rho d\alpha]\, dh}{\pi S^2 a} \quad (10)$$

Therefore, the detector efficiency using perpendicular cylindrical sources can be calculated using the efficiency transfer principle as follow:

$$\varepsilon(E, Cyl\text{-}Per) = \varepsilon(E, Point)\frac{\Omega_{eff\ (Cyl\text{-}Perl)}}{\Omega_{eff(Point)}} \quad (11)$$

where, $\varepsilon_{(E,Cyl\text{-}Per)}$ and $\varepsilon_{[E,Point]}$ are the full-energy peak efficiency of the cylindrical detector, using perpendicular cylindrical radioactive source located at certain position from the detector surface

and an axial point source located at another certain position from the detector surface as a reference geometry, respectively. While $\Omega_{\text{eff (Cyl-Perl)}}$ and $\Omega_{\text{eff(Point)}}$ are the effective solid angles subtended by the detector surface at each source position respectively. The values of the effective solid angle were calculated by using the numerical computation of the double integrals which performed by using the trapezoidal rule. A computer program is designed to calculate the effective solid angle of the detector with respect the both kinds of sources.

EXPERIMENTAL SETUP

In the present work two different types of NaI(Tl) scintillation detectors were used. These detectors takes the abbreviations D1 and D2 for the 2"x2" and 3"x3" inches detectors. The experimental measurements were performed for two types of radioactive sources. The point sources are ^{241}Am, ^{133}Ba, ^{152}Eu, ^{137}Cs, and ^{60}Co which purchased from the Physikalisch-Technische Bundesanstalt (PTB) in Braunschweig and Berlin. The sources activities and their uncertainties are listed in Table (1). Half-lifes, photon energies and photon emission probabilities per decay for all radionuclides used in the calibration process were listed in Table (2).

Calibration process was done by using a homemade Plexiglas holder to measure the point sources at four different axial distances starting from approximately 20, 25, 30 and 35 cm from the surface of the two detectors. The holder is placed directly on the detector entrance window as an absorber material to avoid the effect of β- and x- rays and to protect the detector heads. In most cases the accompanying x-ray was soft enough to be absorbed completely before entering the detector [9]. The source-to-detector separations start from 20 cm to neglect the coincidence summing corrections.

Table (1): PTB point sources activities and their uncertainties.

PTB-Nuclide	Activity (kBq)	Reference Date 00:00Hr	Uncertainty(kBq)
^{241}Am	259.0	1.June 2009	±2.6
^{133}Ba	275.3		±2.8
^{152}Eu	290.0		±4.0
^{137}Cs	385.0		±4.0
^{60}Co	212.1		±1.5

Table (2): Half lives, photon energies and photon emission probabilities per decay for the used Point sources.

PTB-Nuclide	Energy (keV)	Emission Probability %	Half Life Day
^{241}Am	59.52	35.9	157861.05
^{133}Ba	80.99	34.1	3847.91
^{152}Eu	121.78	28.4	4943.29
	244.69	7.49	
	344.28	26.6	
	778.9	12.96	
	964.13	14.0	
	1408.01	20.87	
^{137}Cs	661.66	85.21	11004.98
^{60}Co	1173.23	99.9	1925.31
	1332.5	99.982	

The second type of sources was three perpendicular cylindrical sources of dimensions smaller than the scintillation detector dimensions and were filled with ^{152}Eu solution of known activity (V1, V2 and V3). The properties of perpendicular cylindrical sources that used in the study are tabulated in Table (3).

Table (3): The prepared home made radioactive sources detail.

Volume	Activity (kBq)	Nuclide	Reference Date	Uncertainty %	Recording Code	
V1 (20 ml)	4	^{152}Eu	00:00Hr 1.Jan 2010	±1.98	V1D1	V1D2
V2 (25 ml)	5				V2D1	V2D2
V3(50 ml)	5				V3D1	V3D2

These volumetric sources were placed on the detector end-cap and the center of the sources centered with the end-cap. All the spectrums were acquired by winTMCA32 software which made by ICx Technologies. Then it was analyzed by using Genie 2000 data acquisition and analysis software which made by Canberra where the automatic peak search and the peak area calculations were done, along with changes in the peak fit using the interactive peak fit interface when necessary to reduce the residuals and errors in the peak area values [9]. The live time, the run time, and the start time for each spectrum were entered into the spreadsheets. These sheets were used to perform the calculations necessary to generate the experimental (FEPE) curves with their associated uncertainties as a function of the photon energy which listed in Tables 4 and 5. The measured full-energy peak efficiency values started from P4 = 20 cm up to P7 = 35 cm with the associated uncertainties for using point sources and the calculated values based on equation (11) as a function of the photon energy are shown in Figure (2) and (3).

RESULT AND DISCUSSION

This part shows a comparison between the experimental (FEPE) and the Calculated one by using the efficiency transfer theoretical method (ETTM). The experimental work was held at Prof. Dr. Younis. S. Selim laboratory for Radiation Physics, Faculty of Science, Alexandria University, Alexandria, Egypt. The laboratory used several coaxial NaI(Tl) scintillation detectors 2"x2" and 3"x3" inches, which were used in this investigation. The detectors were calibrated by measuring the lowest activity point sources that previously described. The theoretical (FEPE) can be obtained as given in equation (11). The percentage error between the measured and the calculated efficiencies was given by:

$$\Delta\% = \frac{\varepsilon_{ETTM} - \varepsilon_{meas}}{\varepsilon_{meas}} \times 100 \qquad (12)$$

where ε_{cal} and ε_{meas} are the calculated and experimentally measured efficiencies, respectively. The full-energy peak efficiency values for all NaI Scintillation detectors were measured as a function of the photon energy and calculated using the following equation:

$$\varepsilon(E) = \frac{N(E)}{T \cdot A_S \cdot P(E)} \prod C_i \qquad (13)$$

where N(E) was the number of counts in the full-energy peak and it can be obtained by using Genie 2000 software, T was the measuring time (in second), P(E) was the photon emission probability at energy E, A_S was the radionuclide activity, and C_i, where the correction factors due to dead time and radionuclide decay.

For the measurements of the low activity sources, the dead time had been always less than 3%, so the corresponding factor was obtained simply using ADC live time. The statistical uncertainties of the net peak areas were smaller than 1.0 %. Since the acquisition time was long enough to get the number of counts which was at least 10,000 counts. Therefore, the background subtraction was done. The decay correction C_d for the calibration source from the reference time to the run time was given by:

$$C_d = e^{\lambda \cdot \Delta T} \qquad (14)$$

where λ is the decay constant and ΔT is the time interval over which the source decays corresponding to the run time. The main source of uncertainty in the efficiency calculations was the

uncertainties of the activities of the standard source solutions. The coincidence summing effects were negligible in the reference measurement geometries. The uncertainty in the (FEPE) σ_ε was given by:

$$\sigma_\varepsilon = \varepsilon \cdot \sqrt{\left(\frac{\partial \varepsilon}{\partial A}\right)^2 \cdot \sigma_A{}^2 + \left(\frac{\partial \varepsilon}{\partial P}\right)^2 \cdot \sigma_P{}^2 + \left(\frac{\partial \varepsilon}{\partial N}\right)^2 \cdot \sigma_N{}^2} \qquad (15)$$

where σ_A, σ_P, and σ_N, are the uncertainties associated with the quantities A_S, P(E), and N(E), respectively.

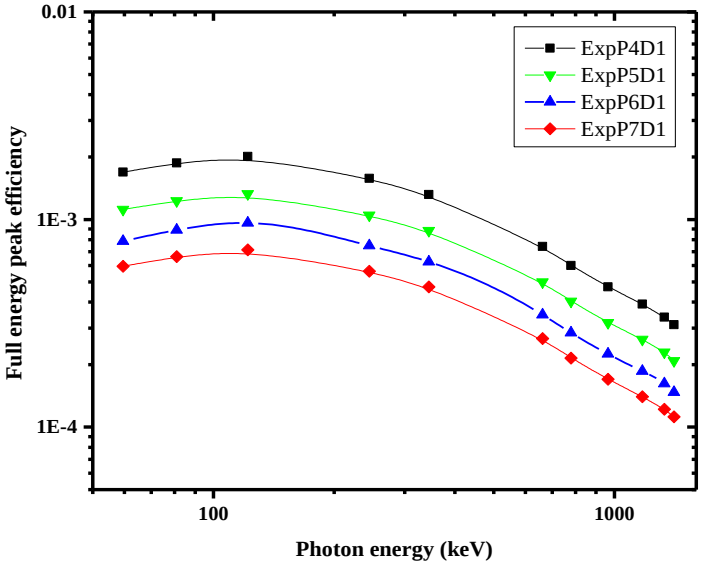

Fig. (2): The measured full-energy peak efficiency values started from P4 = 20 cm up to P7 = 35 cm measured with detector (D1) and the calculated values as a function of the gamma-ray energy at the same positions.

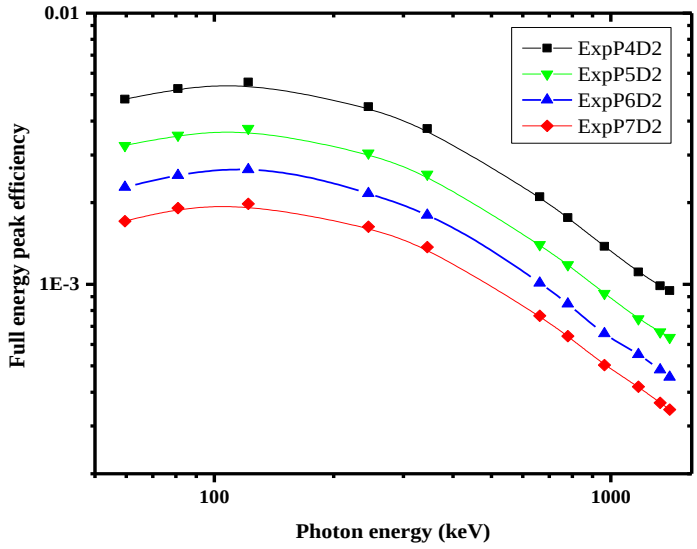

Fig.(3): The measured full-energy peak efficiency values started from P4 = 20 cm up to P7 = 35 cm measured with detector (D2) and the calculated values as a function of the gamma-ray energy at the same positions.

Table (4): Theoretical and Experimental full Energy peak efficiency values for the detector D1 with the discrepancy percentage Δ% between them**.**

Nuclide	Energy	V1D1	P4V1D1		P5V1D1		P6V1D1		P7V1D1	
			ETTM	Δ%	ETTM	Δ%	ETTM	Δ%	ETTM	Δ%
Am-241	59.53		7.60E-02		7.53E-02		7.62E-02		7.44E-02	
Ba-133	80.99		8.21E-02		8.10E-02		8.38E-02		8.10E-02	
Eu-152	121.78	9.16E-02	8.73E-02	-4.75%	8.64E-02	-5.75%	8.87E-02	-3.15%	8.62E-02	-5.94%
Eu-152	244.69	6.49E-02	6.77E-02	4.41%	6.77E-02	4.38%	6.83E-02	5.26%	6.76E-02	4.22%
Eu-152	344.28	5.31E-02	5.60E-02	5.43%	5.62E-02	5.89%	5.63E-02	6.13%	5.61E-02	5.58%
Cs-137	661.66		3.11E-02		3.14E-02		3.08E-02		3.12E-02	
Eu-152	778.9	2.33E-02	2.52E-02	8.18%	2.53E-02	8.56%	2.52E-02	8.17%	2.51E-02	8.00%
Eu-152	964.13	1.84E-02	1.98E-02	7.62%	1.99E-02	8.61%	1.98E-02	7.93%	1.97E-02	7.55%
Co-60	1173.23		1.63E-02		1.65E-02		1.64E-02		1.62E-02	
Co-60	1332.5		1.41E-02		1.43E-02		1.42E-02		1.41E-02	
Eu-152	1408.01	1.25E-02	1.29E-02	3.10%	1.30E-02	3.71%	1.29E-02	2.92%	1.29E-02	3.32%
Nuclide	**Energy**	**V2D1**	**P4V2D1**		**P5V2D1**		**P6V2D1**		**P7V2D1**	
			ETTM	**Δ%**	**ETTM**	**Δ%**	**ETTM**	**Δ%**	**ETTM**	**Δ%**
Am-241	59.53		7.21E-02		7.14E-02		7.23E-02		7.06E-02	
Ba-133	80.99		7.79E-02		7.69E-02		7.96E-02		7.69E-02	
Eu-152	121.78	8.98E-02	8.29E-02	-7.65%	8.20E-02	-8.62%	8.43E-02	-6.11%	8.19E-02	-8.81%
Eu-152	244.69	6.15E-02	6.40E-02	3.94%	6.40E-02	3.92%	6.45E-02	4.79%	6.39E-02	3.75%
Eu-152	344.28	5.29E-02	5.33E-02	0.79%	5.35E-02	1.23%	5.36E-02	1.46%	5.34E-02	0.93%
Cs-137	661.66		2.97E-02		2.99E-02		2.94E-02		2.98E-02	
Eu-152	778.9	2.29E-02	2.40E-02	4.79%	2.41E-02	5.16%	2.40E-02	4.78%	2.40E-02	4.61%
Eu-152	964.13	1.79E-02	1.88E-02	5.05%	1.90E-02	6.02%	1.89E-02	5.36%	1.88E-02	4.99%
Co-60	1173.23		1.56E-02		1.57E-02		1.56E-02		1.55E-02	
Co-60	1332.5		1.35E-02		1.36E-02		1.35E-02		1.35E-02	
Eu-152	1408.01	1.16E-02	1.23E-02	5.94%	1.24E-02	6.56%	1.23E-02	5.74%	1.24E-02	6.16%
Nuclide	**Energy**	**V3D1**	**P4V3D1**		**P5V3D1**		**P6V3D1**		**P7V3D1**	
			ETTM	**Δ%**	**ETTM**	**Δ%**	**ETTM**	**Δ%**	**ETTM**	**Δ%**
Am-241	59.53		5.89E-02		5.84E-02		5.91E-02		5.77E-02	
Ba-133	80.99		6.48E-02		6.39E-02		6.61E-02		6.39E-02	
Eu-152	121.78	7.58E-02	6.98E-02	-7.90%	6.90E-02	-8.86%	7.09E-02	-6.36%	6.89E-02	-9.05%
Eu-152	244.69	5.61E-02	5.47E-02	-2.54%	5.47E-02	-2.57%	5.51E-02	-1.75%	5.46E-02	-2.72%
Eu-152	344.28	4.46E-02	4.59E-02	2.80%	4.61E-02	3.25%	4.62E-02	3.48%	4.59E-02	2.95%
Cs-137	661.66		2.59E-02		2.61E-02		2.56E-02		2.60E-02	
Eu-152	778.9	1.98E-02	2.10E-02	6.03%	2.11E-02	6.40%	2.10E-02	6.02%	2.10E-02	5.85%
Eu-152	964.13	1.59E-02	1.66E-02	4.08%	1.67E-02	5.03%	1.66E-02	4.38%	1.65E-02	4.02%
Co-60	1173.23		1.37E-02		1.39E-02		1.38E-02		1.36E-02	
Co-60	1332.5		1.19E-02		1.20E-02		1.19E-02		1.19E-02	
Eu-152	1408.01	1.05E-02	1.09E-02	3.87%	1.10E-02	4.49%	1.09E-02	3.68%	1.09E-02	4.09%

Table (5): Theoretical and Experimental full Energy peak efficiency values for the detector D2 with the discrepancy percentage Δ% between them.

Nuclide	Energy	V1D2	P4V1D2		P5V1D2		P6V1D2		P7V1D2	
			ETTM	Δ%	ETTM	Δ%	ETTM	Δ%	ETTM	Δ%
Am-241	59.53		1.31E-01		1.31E-01		1.31E-01		1.29E-01	
Ba-133	80.99		1.43E-01		1.43E-01		1.43E-01		1.43E-01	
Eu-152	121.78	1.42E-01	1.52E-01	6.41%	1.52E-01	6.60%	1.51E-01	6.11%	1.49E-01	4.91%
Eu-152	244.69	1.16E-01	1.24E-01	7.23%	1.24E-01	7.24%	1.24E-01	7.07%	1.23E-01	6.79%
Eu-152	344.28	9.88E-02	1.03E-01	4.55%	1.04E-01	5.41%	1.03E-01	4.72%	1.04E-01	5.62%
Cs-137	661.66		5.81E-02		5.77E-02		5.83E-02		5.87E-02	
Eu-152	778.9	4.88E-02	4.88E-02	0.01%	4.85E-02	-0.58%	4.91E-02	0.46%	4.94E-02	1.24%
Eu-152	964.13	4.09E-02	3.83E-02	-6.44%	3.82E-02	-6.52%	3.82E-02	-6.62%	3.88E-02	-5.18%
Co-60	1173.23		3.09E-02		3.09E-02		3.21E-02		3.24E-02	
Co-60	1332.5		2.75E-02		2.77E-02		2.81E-02		2.82E-02	
Eu-152	1408.01	2.90E-02	2.64E-02	-8.88%	2.64E-02	-8.87%	2.64E-02	-8.81%	2.67E-02	-7.99%
Nuclide	**Energy**	**V2D2**	**P4V2D2**		**P5V2D2**		**P6V2D2**		**P7V2D2**	
			ETTM	**Δ%**	**ETTM**	**Δ%**	**ETTM**	**Δ%**	**ETTM**	**Δ%**
Am-241	59.53		1.12E-01		1.12E-01		1.11E-01		1.10E-01	
Ba-133	80.99		1.25E-01		1.25E-01		1.25E-01		1.25E-01	
Eu-152	121.78	1.33E-01	1.34E-01	0.84%	1.35E-01	1.03%	1.34E-01	0.56%	1.33E-01	-0.57%
Eu-152	244.69	1.07E-01	1.12E-01	4.78%	1.12E-01	4.80%	1.11E-01	4.62%	1.11E-01	4.35%
Eu-152	344.28	9.32E-02	9.37E-02	0.50%	9.45E-02	1.33%	9.39E-02	0.67%	9.47E-02	1.54%
Cs-137	661.66		5.34E-02		5.30E-02		5.35E-02		5.39E-02	
Eu-152	778.9	4.50E-02	4.50E-02	0.03%	4.47E-02	-0.56%	4.52E-02	0.49%	4.55E-02	1.26%
Eu-152	964.13	3.80E-02	3.54E-02	-6.86%	3.53E-02	-6.94%	3.53E-02	-7.03%	3.59E-02	-5.60%
Co-60	1173.23		2.87E-02		2.86E-02		2.98E-02		3.01E-02	
Co-60	1332.5		2.66E-02		2.67E-02		2.71E-02		2.72E-02	
Eu-152	1408.01	2.61E-02	2.46E-02	-5.83%	2.46E-02	-5.83%	2.46E-02	-5.76%	2.48E-02	-4.92%
Nuclide	**Energy**	**V3D2**	**P4V3D2**		**P5V3D2**		**P6V3D2**		**P7V3D2**	
			ETTM	**Δ%**	**ETTM**	**Δ%**	**ETTM**	**Δ%**	**ETTM**	**Δ%**
Am-241	59.53		1.04E-01		1.04E-01		1.04E-01		1.02E-01	
Ba-133	80.99		1.14E-01		1.14E-01		1.15E-01		1.15E-01	
Eu-152	121.78	1.11E-01	1.21E-01	9.18%	1.22E-01	9.38%	1.21E-01	8.87%	1.20E-01	7.65%
Eu-152	244.69	9.38E-02	9.98E-02	6.35%	9.98E-02	6.36%	9.96E-02	6.18%	9.94E-02	5.91%
Eu-152	344.28	8.10E-02	8.34E-02	3.01%	8.41E-02	3.87%	8.36E-02	3.19%	8.43E-02	4.07%
Cs-137	661.66		4.71E-02		4.68E-02		4.73E-02		4.76E-02	
Eu-152	778.9	4.17E-02	3.97E-02	-4.81%	3.94E-02	-5.38%	3.98E-02	-4.38%	4.01E-02	-3.64%
Eu-152	964.13	3.27E-02	3.11E-02	-4.88%	3.11E-02	-4.96%	3.11E-02	-5.06%	3.15E-02	-3.60%
Co-60	1173.23		2.52E-02		2.51E-02		2.61E-02		2.64E-02	
Co-60	1332.5		2.24E-02		2.26E-02		2.29E-02		2.30E-02	
Eu-152	1408.01	2.25E-02	2.15E-02	-4.30%	2.15E-02	-4.30%	2.16E-02	-4.23%	2.18E-02	-3.37%

CONCLUSION

The work led to a simple (ETTM) to evaluate the full-energy peak efficiency over a wide energy range using two detectors, five axial point sources and three perpendicular cylindrical radioactive sources were used, also this work can be extended to different sources of different geometries with different detectors. Inaddition, the present work shows a great possibility for calibration the detectors through the determination of a full-energy peak efficiency curve even in those cases when no standard source is available. The source self-attenuation coefficient was taken into account. Computed results were found to be in good agreement with the experimental data. This work has many applications like measuring the activity of radioactive waste drum, looking for holdup places and for locating leakages from underground pipelines.

REFERENCES

(1) G. Haase, D. Tait, A. Wiechon; Nucl. Instrum. Methods; A336, 206 (1993).

(2) A. M. El-Khatib, A. A. Thabet, M. A. Elzaher, M. S. Badawi, B. A. Salem; Journal of Nuclear Engineering and Technology; 46, 2, 217 (2014).

(3) O. Sima, D. Arnold; Appl. Radiat. Isot; 47, 889 (1996).

(4) T. K. Wang, W. Y. Mar, T. H. Ying, C. H. Liao, C. L. Tseng; Appl. Radiat. Isot; 46, 933 (1995).

(5) T. K.Wang, W. Y. Mar, T. H. Ying, C. H. Tseng, C. H. Liao, M. Y. Wang; Appl. Radiat. Isot; 48, 83. (1997).

(6) S. S. Nafee, M. S. Badawi, A. H. Ahmed; Applied Radiation and Isotopes; 68, No. 9, pp.1809-1815 (2010).

(7) M. M. Gouda, M. S. Badawi, A. M. El-Khatib, M. M. Mohamed, A. A. Thabet and M. I. Abbas; JINST, IOP Science. 10, P03022 (2015).

(8) M. S. Badawi, M. A. Elzaher, A. A. Thabet, A. M. El-Khatib; Appl. Radiat. Isot; 74, 46 (2013).

(9) M. S. Badawi, M. M. Gouda, A. Hamzawy, A. M. El-Khatib and M. I. Abbas (2014), Jokull Journal Vol 64, No. 2.

(10) Y. S. Selim, M. I. Abbas; Egyptian. J. Phys;. 26, 79 (1995).

(11) Y. S. Selim, M. I. Abbas; Radiat. Phys. Chem; 48, 23 (1996).

(12) M. I. Abbas, Y. S. Younis; Nucl. Instrum. Methods A; 480, 651 (2002).

(13) M. I. Abbas; Radiat. Phys. Chem; 60, 3 (2001a).

(14) M. I. Abbas; Appl. Radiat. Isot; 55, 245; (2001b).

(15) M. I. Abbas; Appl. Radiat. Isot; 54, 761 (2001c).

(16) Y. S. Selim, M. I. Abbas, M. A. Fawzy; Radiat. Phys. Chem; 53, 589 (1998).

(17) L. Moens, J. De Donder, Lin Xi-lei, F. De Corte, A. De Wispelaere,A. Simonits, H. Hoste; Nucl. Instr. and Meth; 187, 451 (1981).

(18) L. Moens, F. De Corte, A. Simonits, Lin Xi-lei, A. De Wispelaere, J. De Donder, H. Hoste; Journal of Radioanalytical Chemistry, 70, 1-2, 539 (1982).

(19) D. Radu, D. Stanga, O. Sima; Romanian Reports In Physics; 62, 1, 57 (2010).

(20) M. C. Lepy, *et al.;* EUROMET Action 428:; Report CEA–R– 5894, CEA/Saclay (2000).

(21) M. C. Lepy, *et al.;* Appl. Radiat. Isot., 55, 4, 493 (2001).

(22) K. Debertin, U. Schõtzig; Nucl. Instrum. Meth; 158, 471 (1979).

(23) A. A. Thabet, A. D. Dlabac, S. I. Jovanovic, M. S. Badawi, N. N. Mihaljevic, A. M. El-Khatib, M. M. Gouda, M. I. Abbas; Nuclear Technology & Radiation Protection Vol. 30, No. 1. pp. 35-46 (2015).